Biochemical and Biophysical Research Communications 428 (2012) 395–400

Contents lists available at SciVerse ScienceDirect

Biochemical and Biophysical Research Communications

journal homepage: www.elsevier.com/locate/ybbrc

# Robust *in vitro* affinity maturation strategy based on interface-focused high-throughput mutational scanning

Yasuhiro Fujino [a,b,*], Risako Fujita [a], Kouichi Wada [a], Kotomi Fujishige [a], Takashi Kanamori [b], Lindsey Hunt [c], Yoshihiro Shimizu [b,1], Takuya Ueda [b,*]

[a] Advanced Medical Research Department, Mitsubishi Tanabe Pharma Corporation, 3-16-89 Kashima, Yodogawa-ku, Osaka 532-8505, Japan
[b] The Department of Medical Genome Sciences, Graduate School of Frontier Sciences, The University of Tokyo, FSB-401, 5-1-5, Kashiwanoha, Kashiwa, Chiba 277-8562, Japan
[c] Sapidyne Instruments Inc., 700 W. Diamond St., Boise, ID 83705, USA

ARTICLE INFO

*Article history:*
Received 8 October 2012
Available online 26 October 2012

*Keywords:*
Protein engineering
Affinity maturation
Antibody Fab fragment
Mutation scanning
High-throughput sequencing
Ribosome display

ABSTRACT

Development of protein therapeutics or biosensors often requires *in vitro* affinity maturation. Here we report a robust affinity engineering strategy using a custom designed library. The strategy consists of two steps beginning with identification of beneficial single amino acid substitutions then combination. A high quality combinatorial library specifically customized to a given binding-interface can be rapidly designed by high-throughput mutational scanning of single substitution libraries. When applied to the optimization of a model antibody Fab fragment, the strategy created a diverse panel of high affinity variants. The most potent variant achieved 2110-fold affinity improvement to an equilibrium dissociation constant (Kd) of 3.45 pM with only 7 amino acid substitutions. The method should facilitate affinity engineering of a wide variety of protein–protein interactions due to its context-dependent library design strategy.



## 1. Introduction

Affinity engineering is an essential method for the development of valuable protein reagents and therapeutics. Robust affinity improvement such as >1000-fold is quite a challenge due to the complexity of protein–protein interactions and protein sequence-function relationships [1–3]. Thus, there remains a high expectation that a more simple, robust, and rapid approach will become widely applicable. Virtually all currently available strategies depend on the mutant design-evaluation cycle. At one end there are stochastic libraries combined with protein display technology. The other end is computational design to reduce the time needed for experiments. Drawbacks of these approaches include the laborious experiment or inaccurate energy prediction of the cooperative effect of multiple substitutions.

In between these two extremes, nonstochastic or comprehensive approaches have been reported. These approaches are based on the generally accepted principle: the sum of the binding energy changes derived from single substitutions tends to correlate with the binding energy change derived from the multiple substitution. The strategy largely consists of two steps beginning with identification of beneficial amino acid substitutions in the binding-interface then combination [4,5]. However, the identification of beneficial substitutions from a large number of candidates has previously been a bottleneck.

An alternative way to overcome this bottleneck is mutational scanning, which simultaneously interrogates the fitness of a large number of mutants by DNA sequence analysis. Mutational scanning has been used to analyze the comprehensive energy landscape of the protein–protein interaction interfaces [6,7] and can be greatly accelerated by high-throughput DNA sequencing technology [8,9]. The first application of high-throughput mutational scanning to protein engineering was reported recently in the 5 kDa influenza inhibitor protein [10]. However, the affinity improvement was about 30-fold despite intensive scanning against 50 amino acid positions comprising almost the entire region of the small inhibitor protein [10].

*Abbreviations:* Kd, equilibrium dissociation constant; CDR, complementarity determining region; TNFaR, tumor necrosis factor-alpha receptor; PCR, polymerase chain reactions; PURE system, reconstituted in vitro translation system; Fab-PRD, pure ribosome display in single-chain Fab format; ER, enrichment ratio; ELISA, enzyme linked immunosorbent assay; SPR, surface plasmon resonance; KinExA, kinetic exclusion assay.

* Corresponding authors. Address: Advanced Medical Research Department, Mitsubishi Tanabe Pharma Corporation, 3-16-89 Kashima, Yodogawa-ku, Osaka 532-8505, Japan. Fax: +81 6 6300 2696 (Y. Fujino), fax: +81 4 7136 3642 (T. Ueda).

*E-mail addresses:* Fujino.Yasuhiro@mb.mt-pharma.co.jp (Y. Fujino), ueda@k.u-tokyo.ac.jp (T. Ueda).

[1] Present address: Laboratory for Cell-Free Protein Synthesis, Quantitative Biology Center, RIKEN, 2-2-3, Minatojima-minamimachi, Chuo-ku, Kobe, Hyogo 650-0047, Japan.

0006-291X/$ - see front matter © 2012 Elsevier Inc. All rights reserved.
http://dx.doi.org/10.1016/j.bbrc.2012.10.066

We have independently validated affinity engineering by high-throughput mutational scanning focusing on the binding-interface of a relatively large protein. In this report, we optimized the complementarity determining region (CDR) of a 50 kDa antibody Fab fragment against tumor necrosis factor-alpha receptor (TNFaR). The strategy achieved >2000-fold affinity improvement from a Kd of 7.28 nM to 3.45 pM.

## 2. Materials and methods

### 2.1. Reagents

All PCR reactions were performed with PrimeSTAR Max reagent (TaKaRa). All plasmids in this study were created with In-Fusion advantage system (Clontech). All primers are shown in Supplemental Tables 1–3.

### 2.2. Template plasmids

A template DNA sequence (Supplemental Table 4) encoding parental Fab was created on pBluescript SK+(Stratagene). The amino acid sequences of variable domain of the immunoglobulin heavy chain (VH) and that of the light chain (VL) of parental Fab (Supplemental Table 5) were obtained from the synthetic single-chain Fv library previously reported [11]. The remaining part of the template sequence was from synthesized DNA (GENEART). The template DNA sequence has T7 promoter and Shine-Dalgano sequence. The ribosome stall sequence is comprised of two copies of SecM sequence [12] (AKFSTPVWISQAQGIRAGPP) followed by two stop codons. For construction of combinatorial library, the template plasmid was modified by introducing frameshift mutations in two CDR loops (CDR-L3 and CDR-H3).

### 2.3. Reconstituted in vitro translation system (PURE system)

The standard PURE system was prepared as described previously [13] with some modifications. Release factors (RF1, RF2, RF3, and RRF) were excluded in this study. High quality ribosome was prepared by ammonium sulfate precipitation, hydrophobic chromatography and ultracentrifugation as described previously [14].

### 2.4. Biotinylated bait

Recombinant human TNFαR (TNF RI/TNFRSF1A-Fc, R&D Systems) was dissolved in phosphate-buffered saline at a concentration of 0.5 mg/ml and mixed with final 100 μg/mL of sulfo-NHS-SS-biotin (Pierce). The reaction mixture was incubated at 27 °C for 60 min. The remaining free sulfo-NHS-SS-biotin was removed from the reaction mixture using Zeba Spin Desalting Columns (Pierce).

### 2.5. Construction of scanning library

The scanning regions for single amino acid substitution were highlighted on template sequence in Supplemental Tables 4 and 5. The PCR amplifications from template plasmid were performed to prepare a universal upstream fragment and 50 different downstream fragments. Each downstream fragment was converted to a full-length single substitution library by asymmetric overlap extension PCR with a universal upstream fragment. Single substitution libraries were combined in an equimolar ratio to prepare single substitution scanning libraries.

### 2.6. Construction of combinatorial library

The complete DNA sequence of combinatorial library is shown in Supplemental Table 6. The PCR amplifications from frameshift template plasmid were performed to prepare seven DNA fragments, which were converted to a full-length combinatorial library by overlap extension PCR.

### 2.7. Pure ribosome display in single-chain Fab format (Fab-PRD)

The overview of the procedure is shown in Supplemental Fig. 1. Transcription reactions were performed using T7 RNA polymerase (Invitrogen) with 0.4–2 pmol library DNA. Translation reactions were performed using the PURE system with 2 pmol mRNA and 20 pmol ribosome [13,14]. The translation reaction mixture was diluted 10-fold with WBTBR (50 mM Tris–HCl pH 7.6, 90 mM NaCl, 50 mM $Mg(OAc)_2$, 0.5% Tween20, 5 mg/ml BSA (Sigma), 1.25 mg/ml yeast RNA (Sigma), 0.04 U/μL SUPERase-In (Ambion)). Biotinylated bait was incubated with diluted translation products at 4 °C for 1 h then captured by M-280 streptavidin-coated magnetic beads (Dynal). After washing 3 to 5 times, mRNA was recovered by cleaving the disulfide linkage in the biotinylation reagent with dithiothreitol. The recovered mRNA was converted to cDNA by reverse transcription with superscript III (Invitrogen). The core fragment covering from CDR-L1 to CDR-H3 was amplified by PCR, which was converted to full-length DNA by overlap extension PCR with upstream and downstream DNA fragment.

### 2.8. High-throughput DNA sequencing

The PCR amplifications from initial as well as enriched scanning libraries were performed to prepare the DNA fragments covering the CDR1–CDR3 region of light chain and heavy chain. Each population was amplified using primer with different multiplex identifier tags. After confirmation of PCR product by gel electrophoresis, the 40–60 populations were combined in an equimolar ratio. The combined DNA template was submitted to Hokkaido System Science for emulsion PCR and Roche GS-FLX 454 DNA sequencing. The picotiter plate was divided into 8 physically separated sections using a gasket, and one section equivalent to 100,000 reads was used for the analysis.

### 2.9. Analysis of high-throughput sequencing data

Sequence data from each population were treated identically with custom scripts. All the reads were subjected to the custom filtering process irrespective of average Roche GS-FLX Phred quality scores. The reads of contaminating template DNA, and the reads with insufficient length or frameshift mutation were excluded. The remaining reads were defined as total reads and translated to amino acid sequences. Amino acid sequence data was used to compute frequency of a given single amino acid substitution. Frequency data was used to compute enrichment ratio (ER) of a given single amino acid substitution between successive rounds. The calculation details are shown in Supplemental Doc. 1.

### 2.10. Homology modeling

Several homology models of the parental Fab were built with Discovery Studio 3.1 (Accelrys) using 3E09 (for light chain structure), 2QQK (for heavy chain structure), 2QQK (for VL–VH interface) as templates. A model with compromised loop conformation was selected.

### 2.11. Fab preparation

The core DNA fragments from round-5 selection were cloned into a Fab expression vector. The resulting vector encoding single-chain Fab (scFab) was converted to bicistronic vector expressing natural Fab. The overview of inverse-PCR cloning is shown in Supplemental Fig. 2. Bacterial supernatants were used in enzyme linked immunosorbent assay (ELISA) and surface plasmon resonance (SPR) screening. Affinity purified parental Fab was used for Kd determination by SPR. The periplasmic fraction was used for kinetic exclusion assay (KinExA) measurement. Note that Kd and active Fab concentration can be determined simultaneously in KinExA experiment.

### 2.12. SPR experiment

All SPR experiments were performed at a flow rate of 100 μl/min using ProteOn XPR36 system (BioRad). Biotinylated bait was immobilized on a NLC NeutrAvidin sensor chip.

### 2.13. KinExA experiment

All KinExA experiments were performed at 25 °C using the KinExA 3200 instrument (Sapidyne). The flow rate for all experiments was 0.25 ml/min. TNFαR (TNF RI/TNFRSF1A-Fc; R&D Systems) coated azlactone beads were used as the capture reagent. The free Fab fraction was captured on the beads and detected using DyLight 649-conjugated goat anti-human Fab antibody (Jackson ImmunoResearch Laboratories). For all equilibrium experiments, free TNFαR was 2-fold serially diluted into sample buffer containing a constant Fab concentration. The TNFαR/Fab mixtures were incubated for 48 h to reach equilibrium. The equilibrium titration data were fit to a 1:1 binding model using KinExA Pro software to calculate Kd. The time-resolved method was used to determine $k_{on}$. The exponential decrease of free Fab fraction as a function of time was fit to a reversible bimolecular rate equation to calculate $k_{on}$. The $k_{off}$ was calculated as the product of $k_{on}$ and Kd.

## 3. Results

### 3.1. Interface-focused high-throughput mutational scanning

We focused on 50 amino acid positions comprising six CDR loops (L1, L2, L3, H1, H2, and H3) of parental Fab. A total of 50 single amino acid substitution libraries corresponding to these positions were constructed, each of which replaced the wild-type amino acid with 20 natural amino acids. The single substitution libraries were pooled separately by light chain and heavy chain, resulting in two scanning libraries. The principle of single substitution per Fab is important to interrogate every possible single mutant by small-scale high-throughput mutational scanning and to circumvent unpredictable cooperative interactions between substitutions. High-throughput DNA sequencing analysis of the initial libraries resulted in the detection of 288 of the 361 possible substitutions (79% coverage) from 826 light chain reads, and 493 of the 589 possible substitutions (83% coverage) from 1352 heavy chain reads.

The scanning libraries were selected by newly developed Fab-PRD method under varying stringencies and analyzed by high-throughput DNA sequencing. An ER, defined as the frequency of a given single mutant in the selected library divided by those in the initial library, was calculated for every possible single substitution mutant. For single substitution mutant not detected in initial scanning library, the nominal frequency was defined as the inverse number of the total reads of the initial library.

Although the synonymous variants of parental amino acid sequence showed constant ERs under varying selection stringency, we detected a fraction of single substitution mutants with increased ER irrespective of the count in the initial libraries (Fig. 1 and Supplemental Table 7). These high ER single substitution mutants were efficiently highlighted by three-round selection and well correlated among round-3 libraries (Fig. 1).

### 3.2. Energy landscape mapping

An ER heatmap of single amino acid substitution represents a distinctive mutational fingerprint, as well as a comprehensive binding energy landscape of binding-interface. The heatmap suggested that the binding energy surface of the parental Fab would have enough space to be further optimized, and the sparse matrix database, such as alanine scanning database, would not have enough power to optimize this interface efficiently (Fig. 2A). We computed a position-total ER, the sum of the ERs of 19 substitutions at a given position, to highlight mutational hotspots. In addition to the positions that were intolerant to mutation, we identified several mutational hotspots with high preference to substitutions (Fig. 2B). Interestingly, most of the mutational hotspots with position-total ER over 40 were found at the periphery of the binding-interface (Supplemental Fig. 3). The comprehensive energy landscape with single amino acid resolution illustrated the complexity of mutational preference. One end of the fingerprint, Ala-50 position in CDR-L2 showed a specific requirement of glycine. While the other end, Ile-93 position in CDR-L3 exhibited a preference for several substitutions of different chemical properties, which is not easily explained by relationships between side chain characteristics, suggesting that several context-dependent distinct packing scenarios can exist in this position (Fig. 2A).

### 3.3. Combination search

A combinatorial library was designed based on both the ER of individual single amino acid substitutions and the position-total ER. In addition to the heatmap and histogram shown in Fig. 2A and B, a rank-ordered ER of single substitution provides a guide to pick up the candidate substitutions for combinatorial library (Supplemental Fig. 4). We selected a total of 12 amino acid positions, at least one from each CDR loop, focusing primarily on the higher position-total ER and better spatial distribution to avoid too many substitutions in close proximity. These positions were Ser-34 in CDR-L1, Ala-50 in CDR-L2, Tyr-92 and Ile-93 in CDR-L3, Thr-28, Glu-30 and Gly-35 in CDR-H1, Trp-53, Gly-54 and Thr-57 in CDR-H2, Met-100A and Tyr-100B in CDR-H3 (Fig. 2C). At each randomized position, parental residue and high ER substitutions were represented by a tailored codon (Supplemental Table 8). The theoretical diversity of the combinatorial library was $4.8 \times 10^6$ at the amino acid level. A total of five rounds of Fab-PRD selection were performed with gradually decreasing concentrations of biotinylated bait.

### 3.4. Clone screening

Although the library enrichment by Fab-PRD was performed in scFab format, characterization of individual clones was carried out in natural Fab format to exclude potential linker effects. A natural Fab expression library was constructed by inverse-PCR cloning using round-5 libraries selected with 10 and 100 pM bait concentration. The ELISA screening of 92 clones identified 40 hits, which were then subjected to off-rate screening by SPR.

SPR screening demonstrated that the majority of ELISA positive variants achieved dramatic affinity improvement indicated by extremely slow off-rates (Supplemental Table 9). The DNA sequence

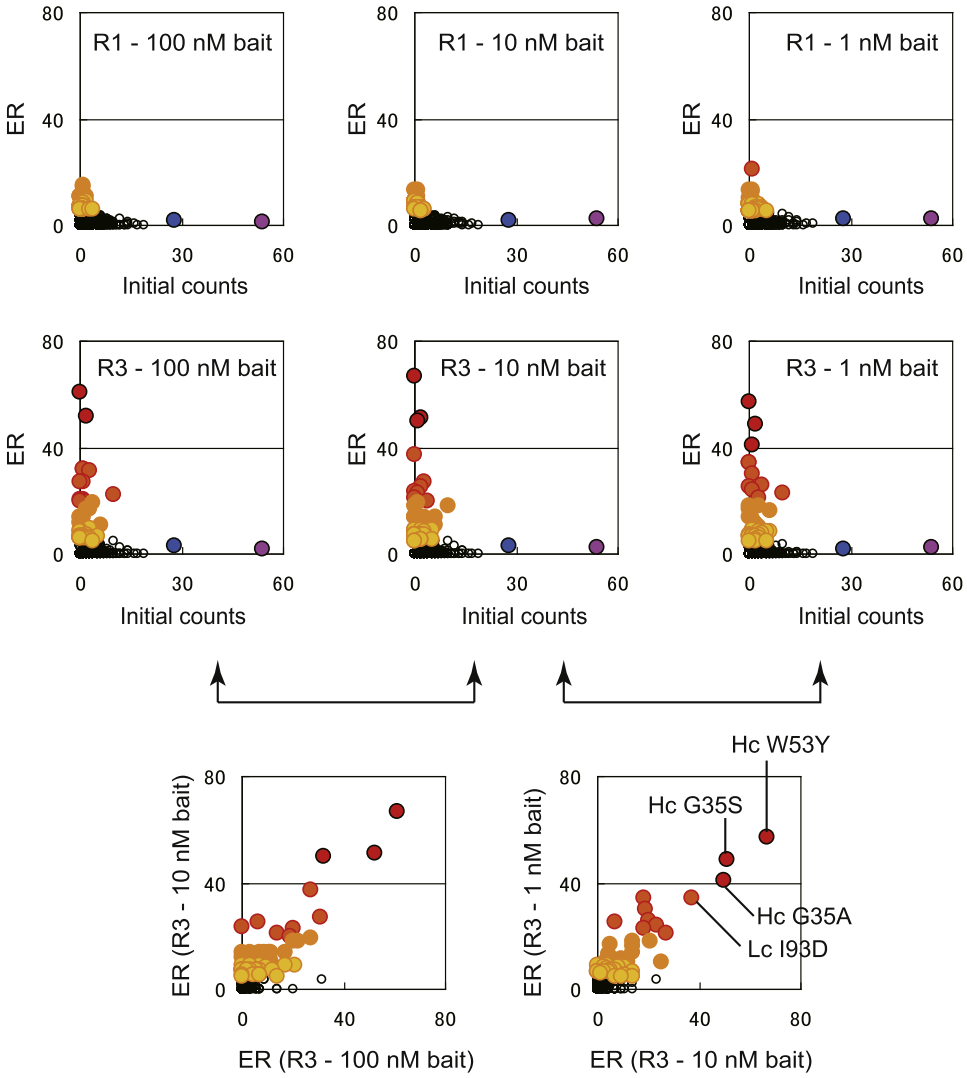


**Fig. 1.** Detection of single amino acid substitution mutants with high ER. (A) The scatter charts of ER versus initial count for every possible 950 single substitution mutant, obtained from high-throughput mutational scanning of either single-round or three-round selected populations with specified bait concentration, are shown. Although the ER of synonymous variants in both the light (light blue) and heavy (purple) chain library are consistently low, a fraction of single mutants with significantly higher ER are detected in round-3 libraries irrespective of the initial count. Each colored dot represents an individual single mutant with ER > 40 (red), ER > 20 (dark orange), ER > 10 (orange), ER > 5 (light orange). (B) The ER versus ER scatter charts between round-3 libraries suggest that detection of high ER single mutants is reproducible. (For interpretation of the references to color in this figure legend, the reader is referred to the web version of this article.)

analysis revealed that each Fab has a different amino acid sequence, so a diverse panel of high affinity Fabs was created (Supplemental Table 9). The off-rates of highly improved binders were too slow to be measured accurately by SPR in a practical time frame due to instrument limitations (Fig. 3A). Affinity measurement of low pM binders by SPR requires strict experimental design to avoid baseline drift, rebinding, mass transport, etc. To avoid these difficulties, kinetic exclusion assay (KinExA) [15] was performed to determine precise affinity.

Three Fabs were selected for KinExA measurement. The Kd of each Fab was determined by equilibrium titration experiment with a wide concentration range of TNFαR into two constant Fab concentrations. Thereby, Kd-controlled (~30 pM Fab) and concentration-controlled (~300 pM Fab) binding curves were collected and globally fit to achieve a dual-curve analysis. Obtained results demonstrated that the Kd of Fab#10 was 18.2 pM, a 400-fold improvement from 7.28 nM of parental Fab. The Kd of Fab#28 was 14.1 pM, achieving 516-fold improvement. The most potent variant was Fab#19 with a Kd of 3.45 pM, a 2110-fold improvement from parental Fab (Fig. 3B). The numbers of substitutions in these Fabs were surprisingly low for the degree of affinity improvement. Fab#10 and Fab#19 had seven substitutions while Fab#28 had five (Table 1).

## 4. Discussion

Most of the previous *in vitro* affinity maturation strategies use stochastic library or predesigned library. Although these strategies have demonstrated significant affinity improvement, they often require laborious and time-consuming processes to achieve even >100-fold affinity improvement [2,16–18]. In addition, affinity improved variants usually acquire more than ten amino acid substitutions. The custom library strategy should be significantly more powerful than previous strategies, because it can effectively counteract the unpredictable binding energy landscape of individual binding-interface and context-dependent properties of mutational tolerance [4,5].

By using a new type of custom library strategy powered by high-throughput DNA sequencing technology, we successfully demonstrated robust affinity improvement with small numbers of substitution from a minimum scale of clone analysis. We cap-

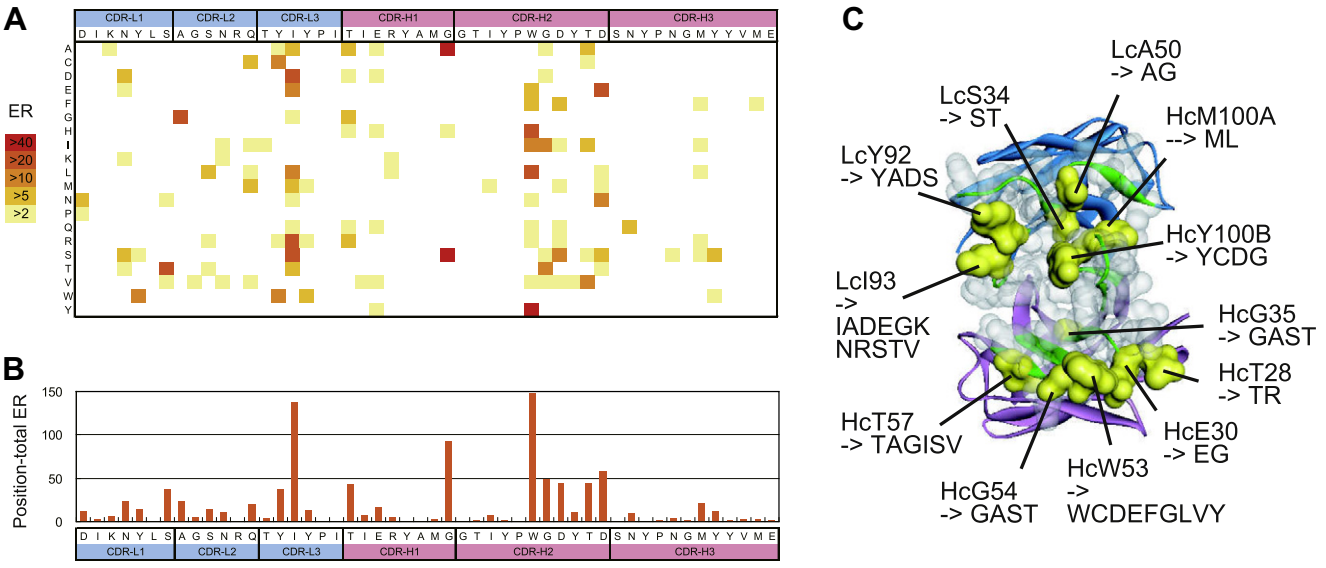


**Fig. 2.** Design of a combinatorial library customized to the binding-interface of parental Fab. (A) A heatmap for ER of every possible 950 single mutant in the scanning library. The map represents a comprehensive energy landscape at single amino acid matrix resolution, indicating which residues are preferred at each position. The data obtained from round-3 library selected with 1 nM bait are shown. (B) A histogram of the position-total ER, the sum of the ER for 19 substitutions at given position, highlights mutational hotspots, most of which were subjected to the randomization in combinatorial library. (C) A total of 12 positions were selected for randomization, at least one from each CDR loop focusing on higher position-total ER as well as good spatial distribution. A tailored degenerate codon was designed to encode high ER substitutions at each position. Design of the combinatorial library are represented on the homology model (top view).

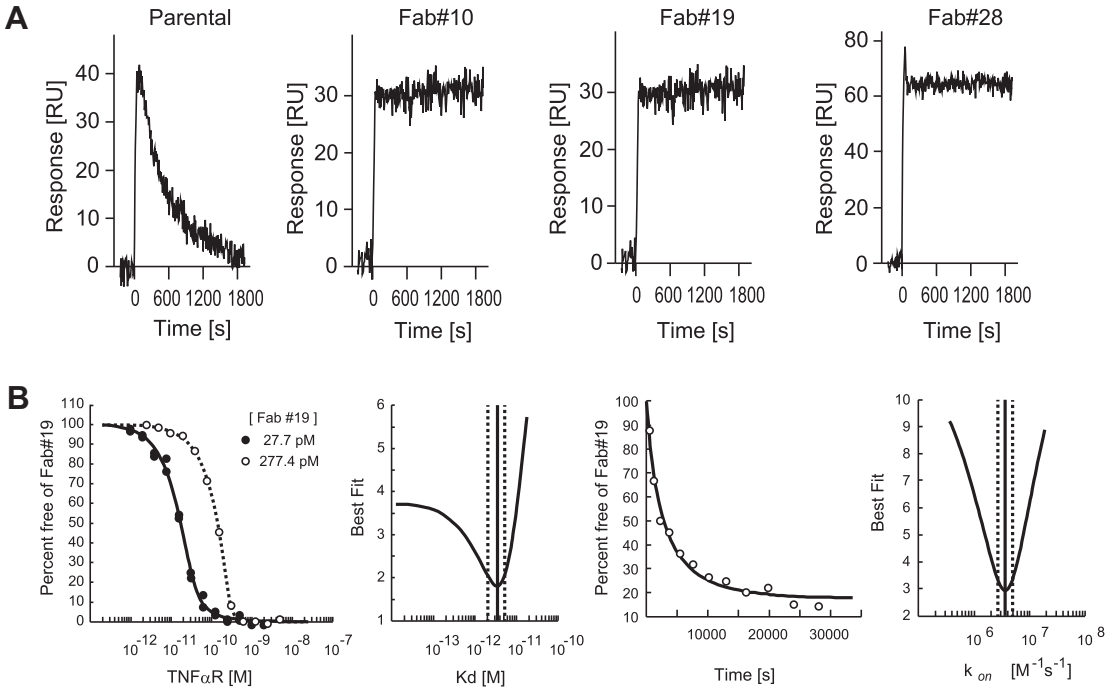


**Fig. 3.** SPR screening and KinExA measurement of affinity engineered Fabs. (A) Comparison of SPR sensorgram for parental Fab and engineered variants demonstrates that clones from the combinatorial library achieved significant improvement in its dissociation profile. The dissociation phase is 30 min. (B) Kd of Fab#19 was determined by KinExA performing equilibrium titration measurements over a wide range of antigen concentrations with two constant Fab#19 concentrations. The dual binding curves were globally fit to a 1:1 binding model, resulting in a Kd of 3.45 pM. The $k_{on}$ was determined using the time resolved method. Equimolar amounts (100 pM) of Fab#19 and antigen were mixed, and the fraction of free Fab#19 was traced until reaching equilibrium.

tured beneficial single amino acid substitutions fulfilling affinity improvement as well as structural requirement by high-throughput mutational scanning of single mutant library. A combinatorial library incorporating these beneficial substitutions is proven to create a convergence of highly optimized binding-interfaces with a minimum number of substitutions. The small substitution number should be due to the simultaneous combinatorial backcross mechanism which eliminates the substitutions that are promising in an ER heatmap as a single substitution, but nonproductive in a combinatorial context.

Fab#10 and Fab#28 achieved similar level of affinity improvement accommodating multiple substitutions in different strategies. Fab#10 simultaneously accommodates three substitutions with ER > 18, suggesting the "parallel-additive" strategy. In con-

**Table 1**
Affinities and binding kinetics of the parental and affinity engineered Fabs. Equilibrium and kinetic parameters for the parental Fab were determined by surface plasmon resonance, and those for engineered variants were obtained by KinExA. Amino acid sequences of these Fabs are shown in Supplemental Table 9.

| Fab | Methods | Kd [M] | $k_{on}$ [$M^{-1}$ $s^{-1}$] | $k_{off}$ [$s^{-1}$] | Relative Kd improvement | Combination-total ER | Number of substitutions |
|---|---|---|---|---|---|---|---|
| Parental | SPR | $7.28 \times 10^{-9}$ | $3.14 \times 10^{5}$ | $2.29 \times 10^{-3}$ | 1 | 26.5 | 0 |
| Fab#10 | KinExA | $1.82 \times 10^{-11}$ | $1.66 \times 10^{6}$ | $3.02 \times 10^{-5}$ | 400 | 97 | 7 |
| Fab#28 | KinExA | $1.41 \times 10^{-11}$ | $6.06 \times 10^{6}$ | $8.55 \times 10^{-5}$ | 516 | 91 | 5 |
| Fab#19 | KinExA | $3.45 \times 10^{-12}$ | $3.64 \times 10^{6}$ | $1.26 \times 10^{-5}$ | 2110 | 122 | 7 |

trast, Fab#28 use "serial-additive" strategy where HcG35A with ER of 41 is a leading substitution and HcG54T with ER of 18 is a supporting substitution. Fab#19 can be recognized as a superior variant of Fab#28, sharing an identical pair of the leading and supporting substitution. This hypothesis can be further supported by the fact that Fab#19 and Fab#28 share common minor substitution such as LcY92A and HcW53F.

The robust optimization mechanism of Fab#19 is probably due to the combination of parallel-additive strategy onto the basis of serial-additive strategy, which successfully accommodates additional supporting substitutions such as LcI93R and HcT57V.

The recent report of affinity engineering by high-throughput mutational scanning achieved 30-fold affinity improvement based on 50 amino acid position scanning at the scan depth of $10^6$ read per population [10]. Here we achieved >2000-fold affinity improvement by same 50 amino acid position scanning even at the scan depth of $10^2$–$10^3$ read per population, which successfully extend the potential of this engineering strategy. The significant difference in the fold-improvement might be due to the difference between interface-focused scanning and whole protein scanning, or the difference between natural antibody scaffold and artificially created inhibitor protein. Further research is needed to show the true potential of this engineering strategy through the optimization trial of different antibodies or protein scaffolds.

## Acknowledgments

We thank our colleagues at Mitsubishi Tanabe Pharma Corporation, University of Tokyo, and Sapidyne Instruments for comments and suggestions. We especially thank M. Kuroda, S. Maeda, H. Nakakubo, M. Arai, H. Nakamura, T. Ishii, and H. Inoue from Mitsubishi Tanabe Pharma Corporation for the various supports for this program; K. Tsumoto from University of Tokyo for critical review of the manuscript; S. Lackie and T.R. Glass from Sapidyne Instruments for their help with KinExA experiments.

## Appendix A. Supplementary data

Supplementary data associated with this article can be found, in the online version, at http://dx.doi.org/10.1016/j.bbrc.2012.10.066.

## References

[1] A.R. Bradbury, S. Sidhu, S. Dubel, J. McCafferty, Beyond natural antibodies: the power of in vitro display technologies, Nat. Biotechnol. 29 (2011) 245–254.
[2] R. Schier, A. McCall, G.P. Adams, K.W. Marshall, H. Merritt, M. Yim, R.S. Crawford, L.M. Weiner, C. Marks, J.D. Marks, Isolation of picomolar affinity anti-c-erbB-2 single-chain Fv by molecular evolution of the complementarity determining regions in the center of the antibody binding site, J. Mol. Biol. 263 (1996) 551–567.
[3] S.M. Lippow, K.D. Wittrup, B. Tidor, Computational design of antibody-affinity improvement beyond in vivo maturation, Nat. Biotechnol. 25 (2007) 1171–1176.
[4] A. Rajpal, N. Beyaz, L. Haber, G. Cappuccilli, H. Yee, R.R. Bhatt, T. Takeuchi, R.A. Lerner, R. Crea, A general method for greatly improving the affinity of antibodies by using combinatorial libraries, Proc. Natl. Acad. Sci. USA 102 (2005) 8466–8471.
[5] C. Votsmeier, H. Plittersdorf, O. Hesse, A. Scheidig, M. Strerath, U. Gritzan, K. Pellengahr, P. Scholz, A. Eicker, D. Myszka, W.M. Coco, U. Haupts, Femtomolar Fab binding affinities to a protein target by alternative CDR residue co-optimization strategies without phage or cell surface display, MAbs 4 (2012).
[6] F.F. Vajdos, C.W. Adams, T.N. Breece, L.G. Presta, A.M. de Vos, S.S. Sidhu, Comprehensive functional maps of the antigen-binding site of an anti-ErbB2 antibody obtained with shotgun scanning mutagenesis, J. Mol. Biol. 320 (2002) 415–428.
[7] G. Pal, J.L. Kouadio, D.R. Artis, A.A. Kossiakoff, S.S. Sidhu, Comprehensive and quantitative mapping of energy landscapes for protein-protein interactions by rapid combinatorial scanning, J. Biol. Chem. 281 (2006) 22378–22385.
[8] D.M. Fowler, C.L. Araya, S.J. Fleishman, E.H. Kellogg, J.J. Stephany, D. Baker, S. Fields, High-resolution mapping of protein sequence-function relationships, Nat. Methods 7 (2010) 741–746.
[9] A. Ernst, D. Gfeller, Z. Kan, S. Seshagiri, P.M. Kim, G.D. Bader, S.S. Sidhu, Coevolution of PDZ domain-ligand interactions analyzed by high-throughput phage display and deep sequencing, Mol. Biosyst. 6 (2010) 1782–1790.
[10] T.A. Whitehead, A. Chevalier, Y. Song, C. Dreyfus, S.J. Fleishman, C. De Mattos, C.A. Myers, H. Kamisetty, P. Blair, I.A. Wilson, D. Baker, Optimization of affinity, specificity and function of designed influenza inhibitors using deep sequencing, Nat. Biotechnol. 30 (2012) 543–548.
[11] T. Shibui, T. Kobayashi, K. Kanatani, A completely in vitro system for obtaining scFv using mRNA display, PCR, direct sequencing, and wheat embryo cell-free translation, Biotechnol. Lett. 31 (2009) 1103–1110.
[12] H. Muto, H. Nakatogawa, K. Ito, Genetically encoded but nonpolypeptide prolyl-tRNA functions in the A site for SecM-mediated ribosomal stall, Mol. Cell 22 (2006) 545–552.
[13] Y. Shimizu, A. Inoue, Y. Tomari, T. Suzuki, T. Yokogawa, K. Nishikawa, T. Ueda, Cell-free translation reconstituted with purified components, Nat. Biotechnol. 19 (2001) 751–755.
[14] H. Ohashi, Y. Shimizu, B.W. Ying, T. Ueda, Efficient protein selection based on ribosome display system with purified components, Biochem. Biophys. Res. Commun. 352 (2007) 270–276.
[15] C. Bee, Y.N. Abdiche, D.M. Stone, S. Collier, K.C. Lindquist, A.C. Pinkerton, J. Pons, A. Rajpal, Exploring the dynamic range of the kinetic exclusion assay in characterizing antigen-antibody interactions, PLoS One 7 (2012) e36261.
[16] W.P. Yang, K. Green, S. Pinz-Sweeney, A.T. Briones, D.R. Burton, C.F. Barbas 3rd, CDR walking mutagenesis for the affinity maturation of a potent human anti-HIV-1 antibody into the picomolar range, J. Mol. Biol. 254 (1995) 392–403.
[17] E.T. Boder, K.S. Midelfort, K.D. Wittrup, Directed evolution of antibody fragments with monovalent femtomolar antigen-binding affinity, Proc. Natl. Acad. Sci. USA 97 (2000) 10701–10705.
[18] C. Zahnd, S. Spinelli, B. Luginbuhl, P. Amstutz, C. Cambillau, A. Pluckthun, Directed in vitro evolution and crystallographic analysis of a peptide-binding single chain antibody fragment (scFv) with low picomolar affinity, J. Biol. Chem. 279 (2004) 18870–18877.